The effect of adding a new monomer “Phene” on the polymerization shrinkage reduction of a dental resin composite

https://doi.org/10.1016/j.dental.2019.02.006

Abstract

Objective: A new photocurable monomer, "Phene" (N-methyl-bis(ethyl-carbamate-isoproply-α-methylstyryl)amine) was synthesized and incorporated into Bis-GMA/TEGDMA with the aim of reducing polymerization shrinkage without detriment to the physical properties and wearing of the resin composites.

Methods: Phene was synthesized through a 2-step reaction route, and its structure was confirmed by FT-IR and ^{1}H-NMR spectra. Phene was incorporated into Bis-GMA/TEGDMA (50/50,wt/wt) with a series of mass fraction (from 0 wt% to 40 wt%). Experimental resin composites were prepared by mixing 29 wt% of resin matrix to 71 wt% of particulate-fillers. Degree of conversion (DC) was determined by FT-IR analysis. The volumetric shrinkage (VS) was calculated as a buoyancy change in distilled water by means of the Archimedes principle. Polymerization shrinkage-stress (SS) was measured using the tensilometer technique. The flexural strength (FS), modulus (FM), and fracture toughness (FT) were measured using a three-point bending setup. A wear test was conducted with 15000 cycles using a dual-axis chewing simulator. Wear depth was measured by a three-dimensional (3D) non-contact optical-profilometer.

Results: ANOVA analysis showed that when mass fraction of Phene in resin matrix was more than 10 wt%, the obtained resin composite formulation had lower DC, VS and SS than control resin composite ($p<0.05$). In general, the experimental resin composites had comparable FS and FM ($p>0.05$) when the mass fraction of Phene in resin matrix was not more than 20 wt.%. Resin composite with 20 wt% Phene had the lowest wear depth and fracture toughness values.

Conclusions: The overall tested properties prove that including Phene up to 20 wt% into Bis-GMA/TEGDMA resin could be potentially useful in the formulation of low-shrinkage resin composites.

Keywords: shrinkage stress, physical properties, volumetric shrinkage, degree of conversion.

1. Introduction

Resin composites used in dental restorative procedures are materials created from a mixture of methacrylate monomers and silanized inorganic fillers. Bisphenol A glycidyl methacrylate (Bis-GMA), triethylene glycol dimethacrylate (TEGDMA) and urethane dimethacrylate (UDMA), are the most widely used monomers in the dental industry [1-3]. The resin composites formulated with the above-mentioned monomers have characteristics that meet most of the demands for dental applications, such as high degree of monomer conversion and mechanical properties, low solubility and, good esthetic features [1]. However, until now commercially available resin composites still have shortcomings that need to be addressed. Obviously, drawbacks related to polymerization shrinkage and polymerization-induced stress continue to be a clinical problem, contributing to premature failure in resin composite restorations [4,5]. Depending on their formulation, resin composites used in restorative dentistry exhibit volumetric shrinkage ranging from 1% up to 6% [6]. Generally, this property is greatly influenced by the chemical structure of the monomers used. Bis-GMA has a high viscosity that negatively interferes with the degree of monomer conversion [7], therefore, low molecular weight dimethacrylates such as TEGDMA or UDMA are incorporated. However, this methodology has been shown to increases water sorption and polymerization shrinkage [8]. Development of a new polymeric system, differing from the traditional methacrylate systems, has been considered an alternative to produce resin composites with significant improvements. In the last few years, different polymer chemistries such as siloranes, liquid crystals, isobornyl acrylate, and thiol-enes have been proposed for changing the organic matrix of resin composites [9-12]. Among the objectives of introducing new monomer systems is the reduction of

polymerization shrinkage behavior (volumetric shrinkage and shrinkage stress) without sacrificing the physical, surface and handling properties as well as the biocompatibility of conventional resin composite [1]. Polymerization shrinkage behavior of resin composites has been determined to be dependent on several factors, such as rate and extent of the polymerization reaction, double-bond concentration, and the modulus of elasticity of the cured resin composites [6,12,13]. Low double-bond conversion and low double-bond concentration will lead to low volumetric shrinkage [14,15]. A reduced polymerization rate and stiffness of cured resin composites, are a benefit for achieving lower shrinkage stress [12,16]. In our previous research, it was found that the reactivity of double bonds in α-methylstyryl group was lower than a double bond in a methacrylate group, thus the polymerization rate of monomer containing α-methylstyryl groups was much slower than the monomer containing methacrylate group [17], which could delay the gel point during light irradiation and provide sufficient time to release the stress [8]. Therefore, using a α-methylstyryl structure containing monomer with a low double bond concentration could be an effective way to prepare low volumetric shrinkage and shrinkage stress resilient resin composites.

Based on this knowledge and with the goal of finding a new co-monomer that can markedly reduce the polymerization shrinkage behavior of Bis-GMA monomer, our research group has investigated the use of a novel monomer named “Phene” (N-methyl-bis(ethyl-carbamate-isoproply-α-methylstyryl)amine) with an α-methylstyryl structure and high molecular weight (536.7) for formulating experimental photo-polymerizable resin composites. The theoretical action mechanism of Phene is that, Phene’s high molecular weight could provide a low double-bond concentration of resin matrix thereby achieving low volumetric shrinkage. Combined with

the low volumetric shrinkage, the slow polymerization rate of Phene could yield low polymerization stress. Therefore, the purpose of the present study was to evaluate the polymerization shrinkage behavior (volumetric shrinkage and shrinkage stress), physical properties (degree of conversion, water sorption, flexural strength and modulus and fracture toughness) and surface properties (microhardness and wear) of a novel experimental resin composite. The null hypotheses were: (1) experimental resin composites will have a similar degree of conversion and lower shrinkage behavior compared to conventional resin composite; (2) experimental resin composites will achieve similar material properties compared to conventional resin composite.

2. Materials and methods

2.1. Materials

Bis-GMA and TEGDMA were purchased from Esstech Inc. (Essington, PA, USA). Camphoroquinone (CQ), and N,N'-dimethylaminoethyl methacrylate (DMAEMA) were purchased from Sigma-Aldrich (St. Louis, MO, USA). N-methyl diethanol amine (MDEA), dibutyltin dilaurate (DBTDL), and 3-isopropenyl-α,α-dimethylbenzyl isocyanate (IDI) were purchased from Sigma-Aldrich Co. All reagents were used without purification. Silaned $BaAlSiO_2$ filler particles (Ø 0.7µm) were received from Schott (UltraFine, Schott, Landshut, Germany).

2.2. Synthesis of "Phene" (N-methyl-bis(ethyl-carbamate-isoproply-α-methylstyryl)amine)

Phene was synthesized according to the route presented in Figure 1. A mixture of MDEA (0.05 mol), IDI (0.10 mol), 100 mL of extra dry acetone, and 2 droplets of DBTDL catalyst were stirred at 45℃. The reaction was continued until the reaction between IDI's isocyanate group and MDEA's hydroxyl group was completed. The completion of the reaction was confirmed by FT-IR. The disappearance of the infrared absorbance peak of the -NCO group (2270 cm^{-1}) in the FT-IR spectra of the samples taken from the reaction medium was observed when the reaction was complete. After removing the acetone by distillation under vacuum, the product was washed with diethyl ether to remove the catalyst. Then the diethyl ether was evaporated from the yellow viscose liquid by drying it in vacuum at 35℃ for 24 h to obtain Phene. The correctness of the chemical structure was confirmed by spectroscopic evaluations FT-IR (Figure 2) and ^{1}H-NMR (Figure 3). The results of spectroscopic studies for Phene were as follows: IR (neat): ν (cm^{-1}) 3340, 2972, 2852, 2800, 1729, 1630, 1600, 1526, 1459, 1230, 1172, 1099, 895. ^{1}H-NMR ($CDCl_3$,

600 MHz): δ 7.40, 7.19-7.25, 5.26, 4.99-5.00, 4.02, 2.59, 2.27, 2.07, 1.57.

2.3. Preparation of experimental dental resin composites

Resin matrices of resin composites were prepared according to the formulations shown in Table 1. All compounds were weighed and mixed under magnetic stirring. Experimental resin composites were prepared by mixing each resin matrix with fillers in a high-speed mixing machine (SpeedMixer, DAC150 FVZ-K, Hauschild, Germany) with a speed of 1900 rpm. The mass ratio between the resin's matrix and fillers was 2/5 (wt/wt).

2.4. Double bond conversion

Double bond conversion (DC%) during and after the photoinitiation of polymerization was monitored by Fourier transform infrared spectroscopy (FT-IR) (Spectrum One, Perkin-Elmer, Beaconsfield Bucks, UK) with an attenuated total reflectance (ATR) accessory. Resin composites were analyzed in a mold that was 1.5 mm thick and 4.5 mm in diameter. First, the spectrum of the unpolymerized sample was placed in the mold and measured. Then the sample was irradiated through an upper glass slide for 40 s with a visible light-curing unit (Elipar TM S10, 3M ESPE, Germany) producing an average irradiance of 1600 mW/cm^2 (Marc Resin Calibrator, BlueLight Analytics Inc., Canada). The sample was scanned for its FT-IR spectrum after being irradiated. The DC was calculated from the aliphatic C=C peak at 1636 cm^{-1} and normalized against the carbonyl C=O peak at 1720 cm^{-1} according to the formula

$$DC = \frac{(A_{c=c} / A_{c=o})_0 - (A_{c=c} / A_{c=o})_t}{(A_{c=c} / A_{c=o})_0} \times 100\%$$

where $A_{C=C}$ and $A_{C=O}$ were the absorbance peak area of methacrylate C=C at 1636 cm^1 and carbonyl at 1720 cm^{-1}, respectively; $(A_{C=C}/A_{C=O})0$ and $(A_{C=C}/A_{C=O})_t$ represented the normalized absorbency of the functional group at the radiation time of 0 and t, respectively; DC is the

conversion of methacrylate C=C as a function of radiation time. For each resin composite, five trials were performed.

2.5. Volumetric shrinkage measurement

The specimens' densities (n=3) were measured to determine volume shrinkage according to Archimedes' principle with a commercial density determination kit of the analytical balance (XS105, Mettler Toledo, Greifensee, Switzerland). The mass of the specimen was weighed in air and water, and density was calculated according to the equation

$$D = \frac{M_1 \times D_w}{M_1 - M_2}$$

where D is the density of the sample, M_1 is the mass of the sample in air, M_2 is the mass of the sample in water, and D_w is the density of water at the measured temperature. For each composite, six trials were performed respectively to calculate the densities of

polymerized and unpolymerized samples. The volumetric shrinkage (VS) was expressed in % and calculated from the densities according to the equation

$$VS = \frac{D_c - D_u}{D_c} \times 100\%$$

where D_u is the density of the unpolymerized sample and D_c is the density of the polymerized sample.

2.6. Shrinkage-stress measurement

Glass fiber-reinforced composite (FRC) rods 4 mm diameter and 4 cm in length, had one of their flat surfaces ground with 180 grit silicon carbide sand paper. Two FRC rods were attached tightly to a universal testing machine (model LRX, Lloyd Instruments Ltd., Fareham, England) and resin composite was applied between the FRC rod surfaces. The height of the specimen was set at 2

mm. Two light units (Elipar TM S10, 3M ESPE, Germany) were used simultaneously for 20 s with the tips in close contact with the resin compsite specimen from both sides. Contraction forces were monitored for 5 min at room temperature (22 °C). Shrinkage stress was calculated by dividing the shrinkage force by the cross-section area of the FRC rod. The maximum shrinkage stress (PS) value was taken from the plateau at the end of the shrinkage stress/time curve. Five specimens were tested for each experimental resin composite.

2.7. Mechanical tests

Three-point bending test specimens ($2 \times 2 \times 25$ mm^3) were made from each resin composite. Bar-shaped specimens were made in half-split stainless steel molds between transparent Mylar sheets. Polymerization of the resin composites was done using a hand light-curing unit (Elipar TM S10, 3M ESPE, Germany) for 20 s in five separate overlapping portions from both sides of the metal mold. The wavelength of the light was between 430 and 480 nm and light intensity was 1600 mW/cm^2. The specimens from each resin composite (n=8) were either stored dry (for one day) or in water (for 30 days) at 37°C before testing. The three-point bending test was conducted according to the ISO 4049 (test span: 20 mm, cross-head speed: 1 mm/min, indenter: 2 mm diameter). All specimens were loaded into a material testing machine (model LRX, Lloyd Instruments Ltd., Fareham, England) and the load-deflection curves were recorded with PC-computer software (Nexygen 4.0, Lloyd Instruments Ltd., Fareham, England).

Flexural strength (σ_f) and flexural modulus (E_f) were calculated from the following formula (ISO 1992):

$\sigma_f = 3F_mL/(2bh^2)$ $\quad$ $E_f = SL^3/(4bh^3)$

Where F_m is the applied load (N) at the highest point of a load-deflection curve, L is the span length (20 mm), b is the width of test specimens and h is the thickness of test specimens. S is the stiffness (N/m). S=F/d and d represents the deflection corresponding to load F at a point in the straight-line portion of the trace.

Single-edge-notched-beam specimens (2.5 x 5 x 25 mm^3) according to an adapted ISO 20795-2 standard method (ASTM 2005), were prepared to determine fracture toughness. A custom-made stainless steel split mold was used, which enabled the specimen's removal without force. An accurately designed slot was fabricated centrally in the mold extending until its mid-height, which enabled the central location of the notch and optimization of the crack length (x) to be half of the specimen's height. The resin composite was inserted into the mold placed over a Mylar-strip-covered glass slide in one increment. Before polymerization a sharp and centrally located crack was produced by inserting a straight edged steel blade into the prefabricated slot. Polymerization of the resin composite was carried out for 20 s in five separate overlapping portions. The upper side of the mold was covered with a Mylar strip and a glass slide from both sides of the blade, before being exposed to the polymerization light. Upon the removal from the mold, each specimen was polymerized also on the opposite side. The specimens from each group (n=8) were stored dry at 37°C for 24 h before testing. The specimens were tested in three-point bending mode, in a universal material testing machine at a crosshead speed of 1.0 mm/min.

The fracture toughness was calculated using the Equation: K_{max}= [P L / B $W^{3/2}$] f(x),

where: f(x) = 3/2x1/2 [1.99-x (1-x) (2.15-3.93x+2.7x2)] / 2(1+2x) (1-x)3/2 and 0<x<1 with x=a/W. Here P is the maximum load in kilonewtons (kN), L is the span length (20 cm), B is the

specimen thickness in centimeters (cm), W is the specimen width (depth) in cm, x is a geometrical function dependent on a/W and a is the crack length in cm.

2.8. Two-body wear

Two specimens of each resin composite were prepared in an acrylic resin block for localized wear testing. Longitudinal cavities (20 mm length x 10 mm width x 3 mm depth) were prepared in the composite blocks and then the resin composites were placed in one increment into the prepared cavities and covered with Mylar strips and glass slides before being light irradiated for 20 s (Elipar TM S10, 3M ESPE, Germany) in five separate overlapping portions. The surfaces were then polished flat using a sequence of #1200- to #4000-grit silicon carbide papers. After one day of water storage (37 °C), a 2-body wear test was conducted using the chewing simulator CS- 4.2 (SD Mechatronik, Feldkirchen-Westerham, Germany) which has two chambers simulating the vertical and horizontal movements simultaneously with water. Each of the chambers consisted of an upper sample holder that can fasten the loading tip (antagonistic) with a screw and a lower plastic sample holder in which the resin composite specimen was embedded. The manufacturer's standard loading tips (Steatite ball, Ø 6 mm) were embedded in acrylic resins in the upper sample holders, and were then fixed with a fastening screw. A weight of 2 kg, which is comparable to 20 N of chewing force and 15,000 loading cycles with frequency of 1.5 Hz were used.

The wear patterns (n=6) on the surface of each specimen were profiled with a 3D optical microscope (Bruker Nano GmbH, Berlin, Germany) using Vision64 software. The maximum wear depth values (µm), representing the average of the lowest or deepest points of all profile scans were calculated from different points.

2.9. Surface microhardness test

Five specimens form each experimental resin composite (2 mm-thick rings with a diameter of 6.5 mm) were prepared. After polymerization, specimens were polished (grit up to 4000 FEPA) at 300 rpm under water cooling using an automatic grinding machine (Steruers Rotopol-11, Copenhagen, Denmark). Specimens were dry stored for 24 h at 37°C before testing. The microhardness of each resin composite was measured using a Struers Duramin hardness microscope (Struers, Copenhagen, Denmark) with a 40 objective lens and a load of 1.96 N applied for 10 s. Each specimen's surface was subjected to 5 indentations. The diagonal length impressions were measured and Vickers values were converted into microhardness values by the machine. Microhardness was obtained using the following equation:

$$H = \frac{1854.4 \times P}{d^2}$$

where H is Vickers hardness in kg/mm^2, P is the load in grams and d is the length of the diagonals in μm.

2.10. Water sorption

Water sorption for each resin composite was measured from three-point bending test specimens (n=8) which were stored in 120 ml of water for 30 days at 37°C. The dry weight (md) of the specimens was measured with a balance (Mettler A30, Mettler Instrument Co., Highstone, NJ, USA), with an accuracy of 0.1 mg. During water immersion, specimen weight (mw) was measured at 1, 2, 3, 4, 10, 14, 28, and 30 days. Water sorption was calculated as follows:

Water sorption % = (mw–md)/md× 100%

2.11. Statistical analysis

The data were statistically analyzed with SPSS version 23 (SPSS, IBM Corp.) using analysis of variance (ANOVA) at the $P<0.05$ significance level followed by a Tukey HSD post hoc test to determine the differences between the groups.

3. Results

The values of DC, VS and SS of the experimental resin composites were listed in Table 2. The results showed that after 40 s of light curing, the control resin composite (Bis-GMA/TEGDMA) and EC-1 had the highest DC value ($p<0.05$) among all of the resin composites (Figure 4). The EC-2, EC-3, and EC-4 had lower and comparable DC values ($p>0.05$). However, DC measurement after 5 min of light curing, showed comparable values (Table 2). The data showed that by increasing the Phene weight ratios, the VS and SS decreased ($p<0.05$). The VS (1.4%) and SS (1 MPa) of EC-4 was the lowest ($p<0.05$) among all experimental resin composites (Table 2, Figure 5). The results of FS and FM were presented in Table 3. All of the experimental resin composites had comparable FS and FM ($p>0.05$) before and after water storage except for EC-3 and EC-4 which revealed a lower FS ($p<0.05$) in dry conditions. A marked decrease in flexural properties (FS and FM) was found for all resin composites after 30 days of water storage (Table 3). Experimental EC-2 resin composite had the lowest ($p<0.05$) fracture toughness (1.27±0.1 MPa $m^{1/2}$) and wear depth (32.5 µm) values among all experimental resin composites (Figures 6 and 7). On the other hand, EC-4 resin composite presented the highest fracture toughness (1.51±0.1 MPa $m^{1/2}$) and wear depth (44.6 µm) values among all resin composites ($p<0.05$). The regression analysis demonstrated a linear relationships between FS values and wear (R^2 =0.7776), KIC and wear (R^2=0.9731), content of Phene and VS (R^2=0.931), and content of Phene and SS (R^2=0.987). As shown in Figure 8, the surface microhardness (VH) decreased as Phene weight ratio increased more than 20 % (EC-3 and EC-4).

The experimental resin composites formulated with Phene exhibited significantly lower water sorption values than control resin composite (Figure 9).

4. Discussion

The structure and chemical properties of monomers have significant influences on the performance of resin composites, thus designing a specific monomer is an effective way to overcome the drawbacks that resin composites have faced. In this study, with the aim of decreasing volumetric shrinkage and shrinkage stress of resin composites, Phene was designed as a high molecular weight monomer with a two α-methylstyryl structure.

Just as expected, volumetric shrinkage and shrinkage stress of resin composites were significantly decreased after incorporation of Phene. The reduction in volumetric shrinkage should be mainly attributed to the higher molecular weight of Phene (536.7) when compared with TEGDMA (286). Because TEGDMA would be replaced by Phene partially after incorporating Phene into a Bis-GMA/TEGDMA resin system, leading to the decrease of double bond concentration of resin composites [18,19].

Consistent with our previous finding [17], resin composites with more Phene had a lower polymerization rate, because the reactivity of double bonds in α-methylstyryl structure was much lower than the double bonds in the methacrylate group [20]. The lower reactivity of Phene might be attributed to its resonance structure which delocalizes the double bonds, thus inhibiting free radical addition reaction. It has been reported that polymerization of α-methylstyryl had an appreciable depropagation rate even at room temperature [21], thus a higher concentration of Phene in a resin matrix would lead to higher probability of depropagation and lower crosslinking density of a polymeric network. In addition to lower volumetric shrinkage, lower polymerization rate and crosslinking density were also a benefit for Phene-containing resin composites to exhibit lower shrinkage stress by delaying the vitrification state of the material [22,23].

In the structure of Phene, there are two benzene groups which can reinforce the physical and mechanical properties [24-27] of resin composites. However, EC-3 and EC-4 had lower FS than the control resin composite when tested in dry conditions. Just as mentioned above, increasing Phene concentration in resin composites would lead to a reduction of crosslinking density, which is also an important factor for physical and mechanical properties of resin composites [24,28]. Therefore, when mass fraction of Phene in a resin matrix was not higher than 20 wt.%, the reinforcement effect of benzene groups was offset by a reduction in crosslinking density, leading to comparable mechanical properties as control group. However, when mass fraction of Phene in resin matrix was increased to 30 wt.% or more, the effect of reduction of crosslinking density dominated, leading to lower mechanical properties than in the control. With the aim of keeping the physical and mechanical properties of resin composites, too much Phene should not be added, even though it has the ability to decrease volumetric shrinkage and shrinkage stress significantly. In this research, adding 20 wt% of Phene to resin matrix of resin composites (EC-2) was the optimal concentration, in order to obtain resin composite with the best comprehensive properties. As regards to flexural strength and modulus, there were no statistically significant differences between the EC-2 experimental resin composite and the control resin composite evaluated before and after water storage. In this study, for all experimental resin composites, the concentrations of filler and initiators were kept constant, so that the significant differences found were attributable mainly to the organic matrix. Several reasons could explain this behavior, especially, the chemical structure of Phene, which has two aromatic rings within its structure, thus a high mechanical resistance and a high resistance to hydrolytic degradation could be expected. However, because of the special polymerization mechanism of α-Methylstyrene [21], abundant Phene would lead to

reduction of crosslinking density of the polymeric network. Therefore, resin composites with 30% and 40% Phene had lower flexural strength. It was interesting to notice that, after water immersion, flexural strength and modulus of resin composites with 30% and 40% Phene became comparable to the control, which meant that reduction rates of flexural strength and modulus were lower for resin composites with 30% and 40% Phene. The reduction of flexural strength and modulus of resin composites were mainly attributed to the absorbed water molecules, which could act as plasticizers to decrease interaction between polymeric chains. Because of higher probability in depropagation of resin composites with large amount of Phene, there might be left several unreacted monomers, which had already acted as plasticizers to decrease flexural strength and modulus before water immersion, thus after water immersion, reduction rates of flexural strength and modulus for resin composites with 30% and 40% Phene were not as high as other resin composites, because the plasticizing effect of unreacted monomers was replaced by the plasticizing effect of water molecules.

On the contrary, the EC-4 resin composite was measured to have the highest fracture toughness values (Figure 6). Fracture toughness correlates to the fracture energy that is consumed in plastic deformation and intended to approximate the crack growth rate [29]. The lower crosslinking density could have an effect on the crack growth behavior, because the fracture energy could be released by the motion of a polymer chain segment, leading to higher fracture toughness values.

One important factor that should be considered in the selection of resin composite in clinical practice is their wear resistance. Interestingly, EC-2 resin composite had the lowest wear depth among all experimental resin composites (Figure 7) and this may be partially attributed to the resiliency of the resin matrix which might offer some shock-absorbing ability. Furthermore, this

study showed good connection between two-body wear and surface hardness, which is in agreement with some literature findings [30,31].

Remarkably, regression analysis demonstrated a positive correlation between flexural strength values and wear results (R^2 =0.7776) and this in accordance with a recent systemic review by Heintze *et al*., who showed moderately positive correlations between clinical wear and laboratory flexural strength outcomes of resin composites [32].

When the resin composites are exposed to or stored in water, two different mechanisms occur. First there will be an uptake of water producing an increased weight (sorption) and leaching or dissolution of components from the material into the mouth (solubility) leading to a reduction in weight [33]. In the present study, control resin composite after 30 days showed a water uptake percentage of 1.4 wt%, which was the highest among all tested materials (Figure. 9). The method of mixing and manipulation of the low viscous resin composite (control) may generate air voids, which may accelerate the water sorption of this group. Air voids incorporated in the resin composite increases the surface exposed to moisture and may lead to inhibition zones with unpolymerized material [34].

The results of this study demonstrated that Phene could be used to reduce volumetric shrinkage and shrinkage stress of resin composites, and similar mechanical properties could be achieved after optimizing the concentration. Because of the appreciable depropagation rate of α-methylstyryl during polymerization, the polymerization mechanism of Phene and how it influences the polymeric network should be investigated to guide further work. Moreover, the properties of Phene containing resin composites, such as water solubility and biocompatibility should also be evaluated in the future to show whether Phene could be used as a potential resin

matrix for resin composites in clinical settings.

5. Conclusion

The use of the monomer Phene up to 20 wt% into Bis-GMA/TEGDMA based resin composite could led to materials with reduced volumetric shrinkage and shrinkage stress without detriment the physical properties and wear resistance of the resin composites. However, incorporation of abundant amounts of Phene would lead to lower double bond conversion.

Acknowledgments

This study belongs to the research activity of BioCity Turku Biomaterials Research Program (www.biomaterials.utu.fi) and it was supported by Stick Tech Ltd. – Member of the GC Group.

Conflicts of Interests

Author SG has received consultancy fees from StickTech / GC

Author PV consults for Stick Tech - Member of the GC Group in R&D and training.

References

[1] Jack L. Ferracane. Resin composites-State of art. Dent Mater 2010;27:29-38.

[2] Garoushi S, Säilynoja E, Vallittu PK, Lassila LVJ. Physical properties and depth of cure of a new short fiber reinforced composite. Dent Mater 2013;29:835-841.

[3] Liu D, Liu F, He J, Lassila LV, Vallittu PK. Synthesis of a novel tertiary amine containing urethane dimethacrylate monomer (UDMTA) and its application in dental resin. J Mater Sci: Mater Med. 2013;24:1595-1603.

[4] Ferracane JL, Hilton TJ. Polymerization stress-is it clinically meaningful? Dent Mater 2016;32:1-10.

[5] van Dijken JW, Lindberg A. A 15-year randomized controlled study of a reduced shrinkage stress resin composite. Dent Mater 2015;31:1150-1158.

[6] Braga RR, Ballester RY, Ferracane JL. Factors involved in the development of polymerization shrinkage stress in resin-composites: A systematic review. Dent Mater 2005;21:962-970.

[7] Sideridou I, Tserki V, Papanastasiou G. Effect of chemical structure on degree of conversion in light-cured dimethacrylate-based dental resins. Biomaterials 2002;23(8):1819-1829.

[8] Wang X, Huyang G, Palagummi SV, Liu X, Skrtic D, Beauchamp C, Bowen R, Sun J. High performance dental resin composites with hydrolytically stable monomers. Dent Mater 2018;34:228-237.

[9] Maghaireh GA, Taha NA, Alzraikat H. The Silorane-based Resin Composites: A Review Oper Dent 2017;42:E24-E34.

[10] Luo S, Zhu W, Liu F, He J. Preparation of a Bis-GMA-Free Dental Resin System with

Synthesized Fluorinated Dimethacrylate Monomers. Int J Mol Sci 2016;17:2014.

[11] Beigi Burujeny S, Atai M, Yeganeh H. Assessments of antibacterial and physico-mechanical properties for dental materials with chemically anchored quaternary ammonium moieties: thiol-ene-methacrylate vs. conventional methacrylate system. Dent Mater 2015;31:244-261.

[12] He J, Garoushi S, Vallittu PK, Lassila LVJ. Effect of low-shrinkage monomers on the physicochemical properties of experimental composite resin. Acta Biomater Odontol Scand 2018;4:30-37.

[13] Schneider LF, Cavalcante LM, Silikas N. Shrinkage stresses generated during resin-composite application: a review. J Dent Biomech 2010;2010:131630.

[14] He J, Liu F, Vallittu PK, Lassila LVJ. Synthesis of dimethacrylates monomers with low polymerization shrinkage and its application in dental composites materials. J Polym Res 2012;19:9932.

[15] Ding Y, Li B, Wang M, Liu F, He J. Bis-GMA free dental materials based on UDMA/SR833s dental resin system. Adv Polym Technol 2016;35:21564.

[16] Magali D, Delphine TB, Jacques D, Gaëtane L. Volume contraction in photocured dental resins: the shrinkage-conversion relationship revisited. Dent Mater 2006;22:359-365.

[17] He J, Söderling E, Lassila LVJ, Vallittu PK. Preparation of antibacterial and radio-opaque dental resin with new polymerizable quaternary ammonium monomer. Dent Mater 2015;31:575-582.

[18] He J, Liao L, Liu F, Luo Y, Jia D. Synthesis and characterization of a new dimethacrylate monomer based on 5,5'-bis(4-hydroxylphenyl)-hexahydro-4,7-methanoindan for root canal

sealer application. J Mater Sci: Mater Med 2010;21:1135-1142.

[19] He J, Luo Y, Liu F, Jia D. Synthesis, characterization and photopolymerization of a new dimethacrylate monomer based on (α-Methyl-benzylidene)bisphenol used as root canal sealer. J Biomat Sci-Polym E. 2010;21:1191-1205.

[20] Liang S, Deng J, Yang W. Monomer reactivity ratio and thermal performance of α-Methyl styrene and glycidyl methacrylate copolymers. Chinese J Polym Sci 2010;28:323-330.

[21] Lowry GG. Radical-initiated homopolymerization of α-Methylstyrene. J Polym Sci 1958;31:187-188.

[22] Lu H, Stansbury JW, Bowman CN. Towards the elucidation of shrinkage stress development and relaxation in dental composites. Dent Mater 2004;20:979-986.

[23] Goncalves F, Pfeifer CCS, Stansbury JW, Newman SM, Braga RR. Influence of matrix composition on polymerization stress development of experimental composites. Dent Mater 2010;26:697-703.

[24] Asmussen E, Peutzfeldt A. Influence of UEDMA, Bis-GMA and TEGDMA on selected mechanical properties of experimental resin composites. Dent Mater 1998;14:51-56.

[25] Moszner N, Salz U. New development of polymeric dental composites. Prog Polym Sci 2001;26:535-576.

[26] Peutzfeldt A. Resin composites in dentistry: The monomer systems. Eur J Oral Sci 1997;105:97-116.

[27] Lovell LG, Stansbury JW, Syrpes DC, Bowman CN. Effects of composition and reactivity on reaction kinetics of dimethacrylate/dimethacrylate copolymerizations. Macromolecules 1999;32:3913-3921.

[28] Silva EM, Miragaya L, Noronha-filho JD, Amaral CM, Poskus LT, Guimarães. Characterization of an experimental resin composite resin composite organic matrix based on a tri-functional methacrylate monomer. Dent Mater J 2016;35:159-165.

[29] Lassila LVJ, Garoushi S, Vallittu PK, Säilynoja E. Mechanical properties of fiber reinforced restorative composite with two distinguished fiber length distribution. J Mech Behav Biomed Mater 2016;60:331–338.

[30] Engelhardt F, Hahnel S, Preis V, Rosentritt M. Comparison of flowable bulk-fill and flowable resin-based composites: an in vitro analysis. Clin Oral Investig. 2016;20:2123-2130.

[31] T Attin, U Koidl, W Buchalla, HG Schaller, AM Kielbassa, E. Hellwig. Correlation of microhardness and wear in differently eroded bovine dental enamel. Arch Oral Biol 1997;42: 243-250.

[32] Heintze SD, Ilie N, Hickel R, Reis A, Loguercio A, Rousson V. Laboratory mechanical parameters of composite resins and their relation to fractures and wear in clinical trials-A systematic review. Dent Mater 2017;33:101-114.

[33] Manuel Toledano, Osorio R, Osorio E, Prati C, Garcia Godoy F. Sorption and solubility of resin based restorative dental materials. J Dent 2003;31:43–50.

[34] Chinelatti AM, Ramos RP, Chimello DT, Palma – Dibb RG. Clinical performance of a resin modified glass-ionomer and two Poly acid modified resin composites in cervical lesions restoration: one year follow up. J Oral Rehabil 2007;31:251–257.

Table 1 Composition of resin matrix for each experimental resin composite

Resin matrix	Components (%)				
	Bis-GMA	TEGDMA	Phene	CQ	DMAEMA
Control	49.3	49.3	0	0.7	0.7
EC-1	44.3	44.3	10	0.7	0.7
EC-2	39.3	39.3	20	0.7	0.7
EC-3	34.3	34.3	30	0.7	0.7
EC-4	29.3	29.3	40	0.7	0.7

Table 2 Double bond conversion (DC), volumetric shrinkage (VS), and shrinkage stress (SS) of experimental resin composites

Composites	DC_{40s} (%)	DC_{5min} (%)	VS (%)	SS (MPa)
Control	63.3 ± 0.6^{a}	65.8 ± 0.4^{a}	3.9 ± 0.9^{a}	4.6 ± 0.4^{a}
EC-1	63.6 ± 1.4^{a}	66.2 ± 1.1^{a}	3.5 ± 0.6^{b}	3.6 ± 0.9^{b}
EC-2	61.3 ± 0.4^{b}	$64.7 \pm 0.3^{a,b}$	2.6 ± 0.7^{c}	3.1 ± 0.2^{b}
EC-3	60.3 ± 0.6^{b}	$64.2 \pm 0.8^{a,b}$	2.6 ± 0.9^{c}	2.1 ± 0.2^{c}
EC-4	59.7 ± 1.6^{b}	63.4 ± 2.0^{b}	1.4 ± 0.6^{d}	1.0 ± 0.2^{d}

DC_{40s}: double bond conversion after 40s of irradiation time.

DC_{5min}: double bond conversion at 5 min after the beginning of irradiation.

[a] The same lowercase letter indicates that there is no statistical difference within a column (Tukey's test, p=0.05)

Table 3 Flexural strength (FS), and flexural modulus (FM) of experimental resin composites

Composites	FS (MPa)		FM (GPa)	
	Before water immersion	After water immersion	Before water immersion	After water immersion
Control	$142 \pm 29^{a,A}$	$108 \pm 22^{a,B}$	$14.5 \pm 1.2^{a,A}$	$11.4 \pm 1.4^{a,B}$
EC-1	$147 \pm 18^{a,A}$	$96 \pm 16^{a,B}$	$14.8 \pm 1.4^{a,A}$	$11.6 \pm 1.4^{a,B}$
EC-2	$159 \pm 14^{a,A}$	$97 \pm 12^{a,B}$	$15.2 \pm 1.0^{a,A}$	$11.9 \pm 3.0^{a,B}$
EC-3	$111 \pm 12^{b,A}$	$101 \pm 21^{a,B}$	$15.1 \pm 1.5^{a,A}$	$11.2 \pm 1.4^{a,B}$
EC-4	$113 \pm 12^{b,A}$	$104 \pm 15^{a,B}$	$15.0 \pm 2.7^{a,A}$	$10.5 \pm 1.8^{a,B}$

[a] The same lowercase letter indicates that there is no statistical difference within a column (Tukey's test, p=0.05)

[A] The uppercase letters indicate statistical differences within FS or FM before and after immersion of the same composite group (Tukey's test, p=0.05)

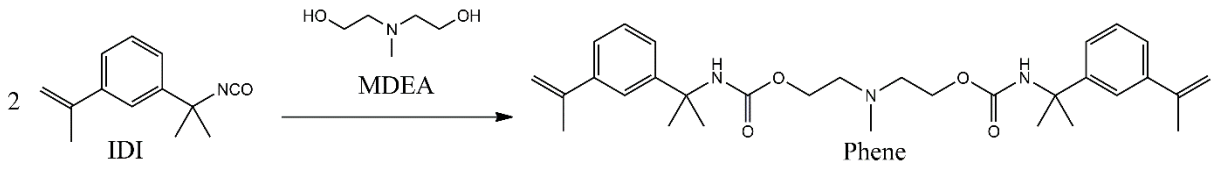

Figure 1. Synthesis route of Phene (N-methyl-bis(ethyl-carbamate-isoproply-α-methylstyryl)-amine) used in this study

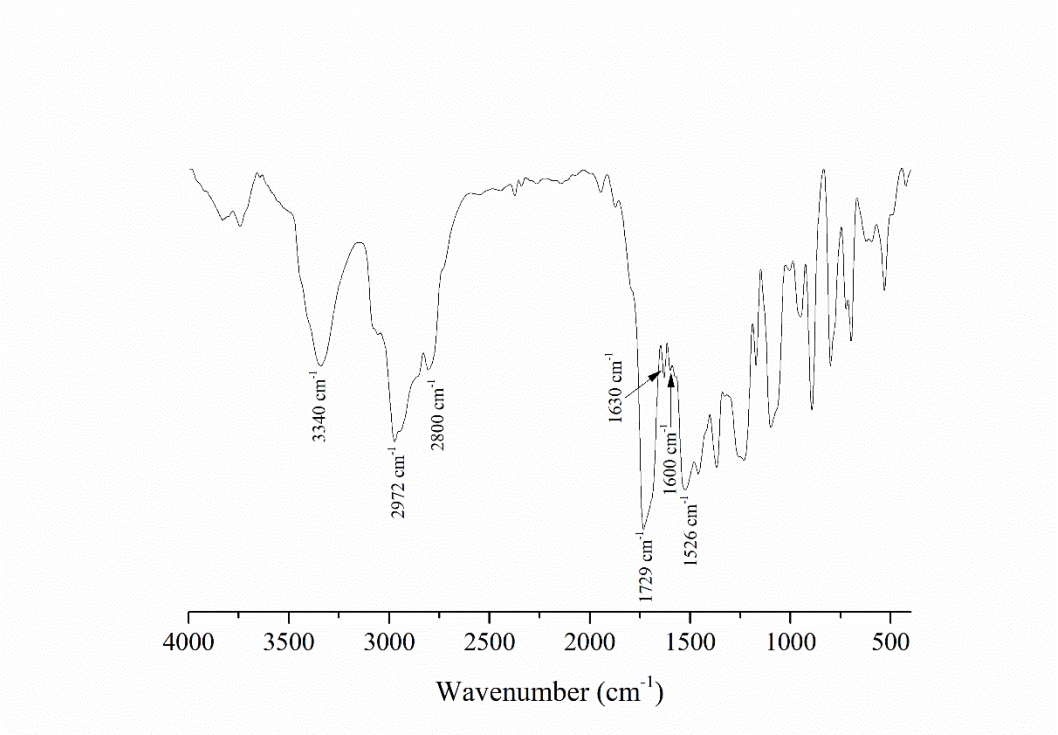

Figure 2. FT-IR spectra of Phene

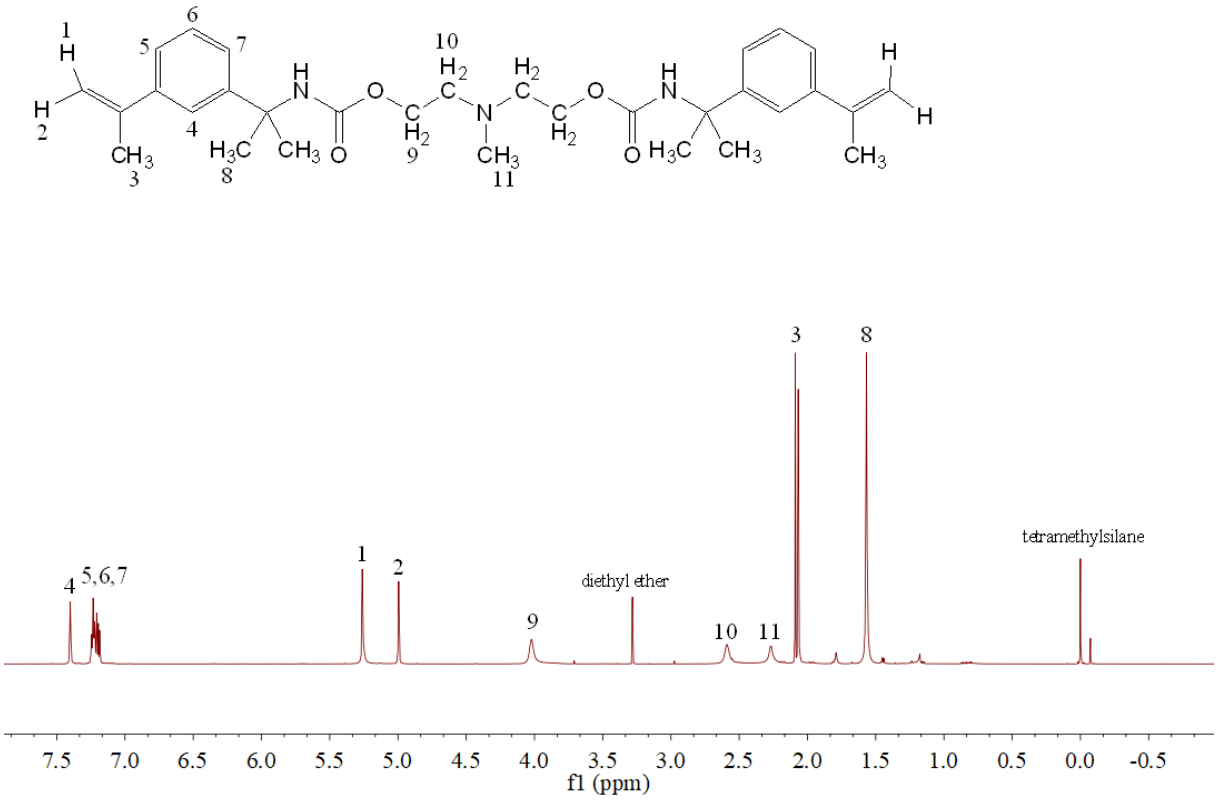

Figure 3. ^{1}H-NMR spectra of Phene

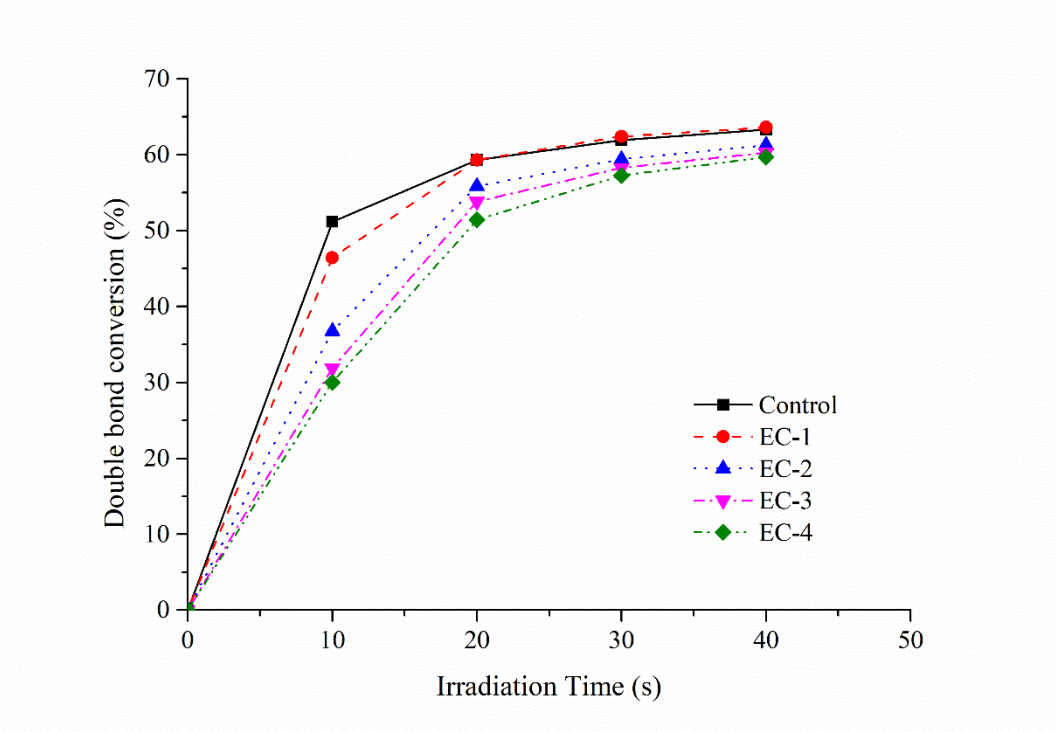

Figure 4. Curves of double bond conversion versus irradiation time of resin composites (Table 1).

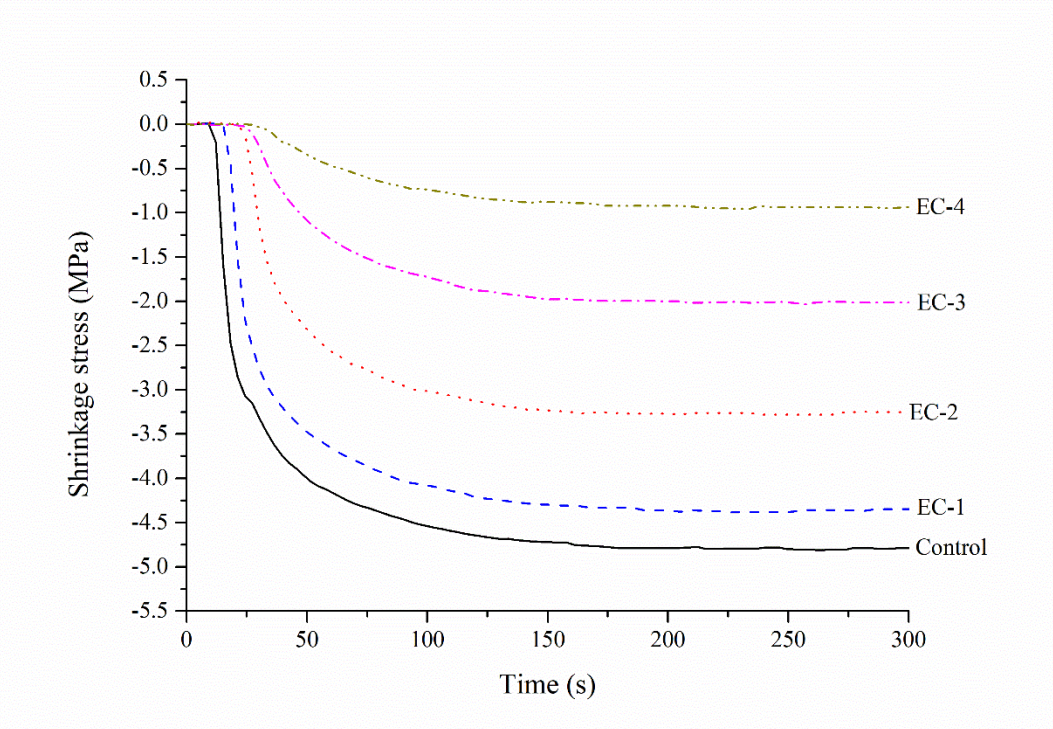

Figure 5. Curves of polymerization shrinkage stress versus time of resin composites (Table 1).

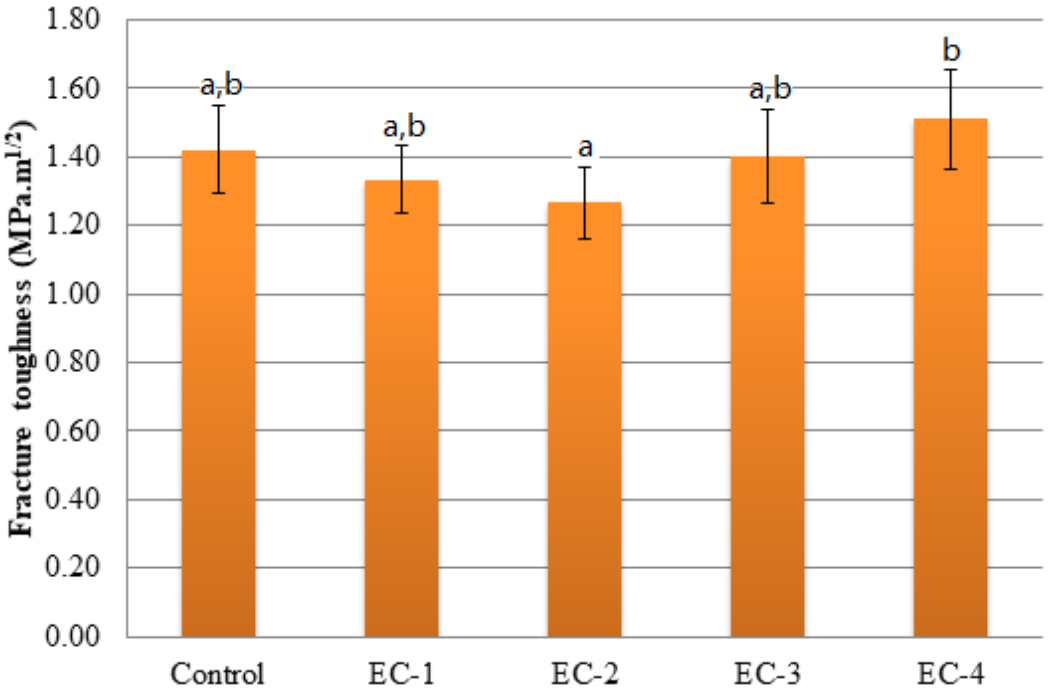

Figure 6. Bar graph illustrating mean fracture toughness (KIC) and standard deviation (SD) of resin composites. The same letters above the bars represent non-statistically significant differences ($p>0.05$) among the groups.

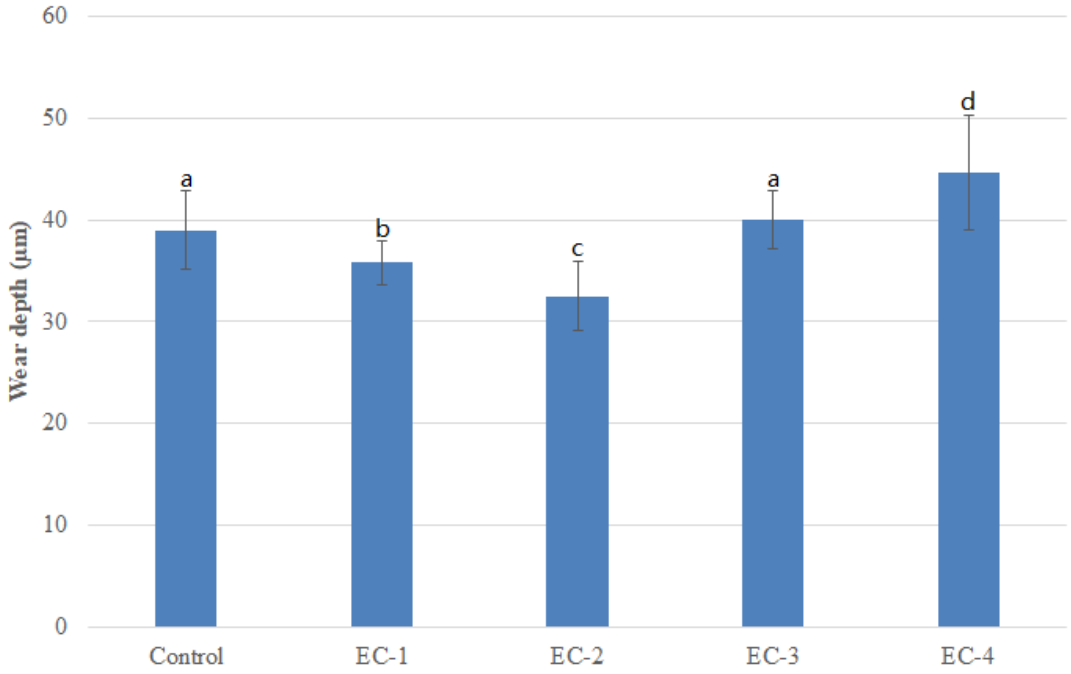

Figure 7. Bar graph illustrating mean wear depth (micron) and standard deviation (SD) of resin composites after 15000 cycles of the 2-body wear test. The same letters above the bars represent non-statistically significant differences ($p>0.05$) among the groups.

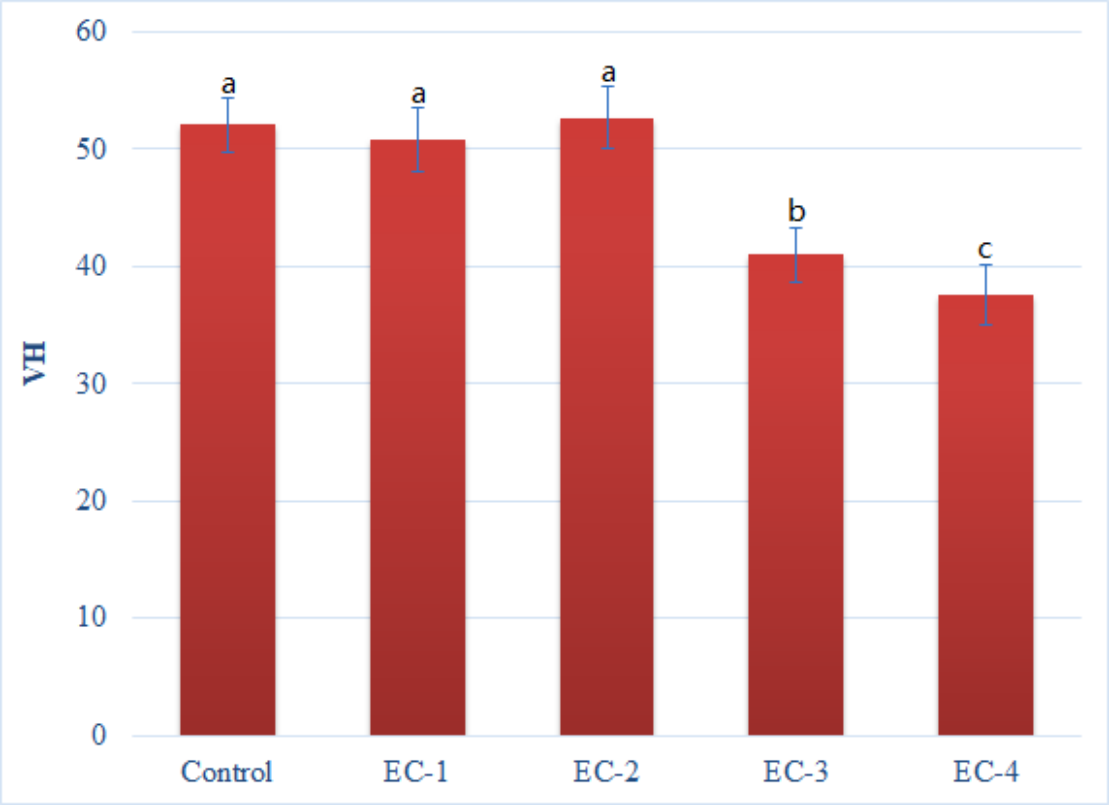

Figure 8. Bar graph illustrating mean microhardness (VH) and standard deviation (SD) of resin composites. The same letters above the bars represent non-statistically significant differences ($p>0.05$) among the groups.

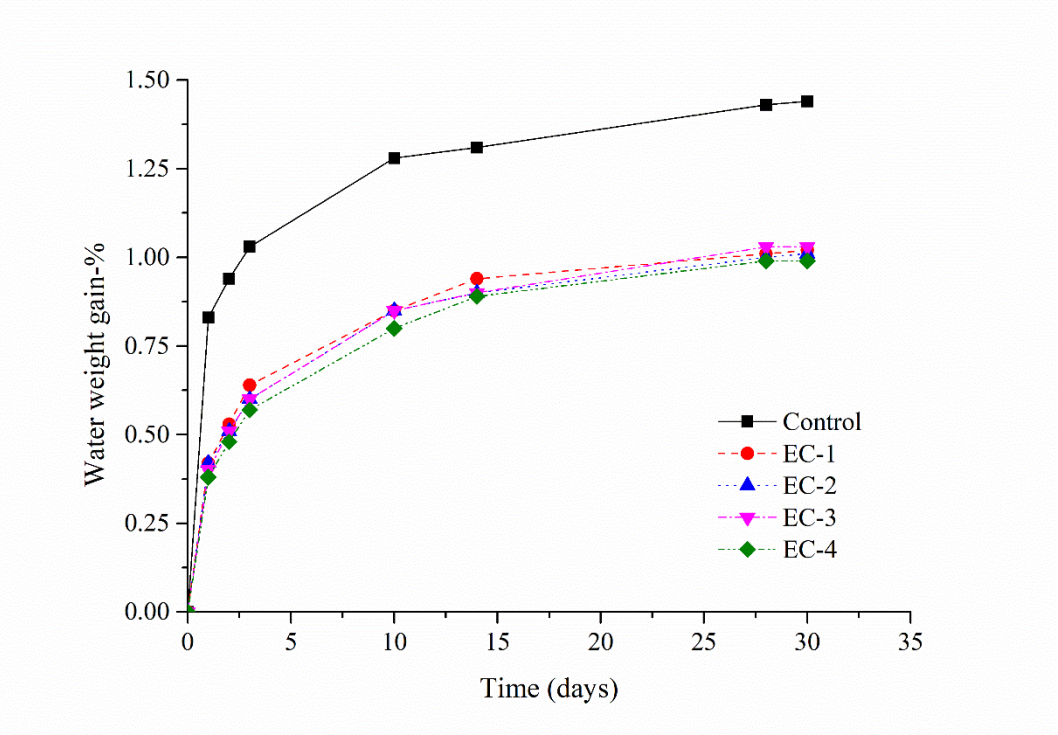

Figure 9. Water sorption (%wt gain) of resin composites during 30 days of storage in water at 37°C